The Solar Gamma Ray and Neutron Capabilities of COMPTEL on the Gamma Ray Observatory

James M. Ryan and John A. Lockwood

Institute for the Study of Earth, Oceans and Space
University of New Hampshire
Durham, NH

Abstract

The imaging Compton telescope COMPTEL on the Gamma Ray Observatory has unusual spectroscopic capabilities for measuring solar γ-ray and neutron emission. The launch of the GRO is scheduled for June 1990 near the peak of the sunspot cycle. With a 30 - 40% probability for the Sun being in the COMPTEL field-of-view during the sunlit part of an orbit, a large number of flares will be observed above the 800 keV γ-ray threshold of the telescope. The telescope energy range extends to 30 MeV with high time resolution burst spectra available from 0.1 to 10 MeV. Strong Compton tail suppression of instrumental γ-ray interactions will facilitate improved spectral analysis of solar flare emissions. In addition, the high signal to noise ratio for neutron detection and measurement will provide new neutron spectroscopic capabilities. Specifically, a flare similar to that of 1982 June 3 will provide spectroscopic data on > 1500 individual neutrons, enough to construct an unambiguous spectrum in the energy range of 20 to 200 MeV. Details of the instrument and its response to solar γ-rays and neutrons will be presented.

1. Introduction

The launch of the Gamma Ray Observatory during the solar maximum in 1990 will provide powerful tools with which to examine the γ-ray and neutron emissions from solar flares. COMPTEL, the imaging double Compton scatter telescope, has unique capabilities for measuring the flux and energy of both the solar γ-ray and neutron emissions. With its field-of-view (FOV) of about 60° for γ-rays and 90° for neutrons, the Sun will be in the field-of-view ~ 40% of the time. In this paper we first describe the detection technique and the physical instrument and then present a preliminary response of COMPTEL to γ-rays and neutrons. Finally, we predict the COMPTEL response to the γ-ray and neutron emissions of the 1982 June 3 solar flare.

2. Compton Telescope Basics

A Compton telescope is a γ-ray detector in which the Compton scattering process is used to measure the photon's energy and incident direction. In this type of detector a γ-ray must scatter in two physically independent detecting elements or planes, nominally a forward and rearward detector. A precise time-of-flight (TOF) measurement establishes the general forward or backward direction of the scattered photon. The measured TOF must be consistent with the light travel time, identifying and, when desired, discriminating against scattered neutrons. Pulse shape discrimination techniques can further isolate the effects of neutrons. This delayed coincidence requirement efficiently suppresses contributions from internal radioactivity and backward scattered particles. These selection criteria can be adjusted to select neutrons, as opposed to photon events, as discussed below. Charged particles are normally rejected via thin active charged particle shields. The Compton scatter kinematics impose an additional geometrical constraint upon the scattering process using the energy deposits in the two detectors to provide the photon scatter angle as described below and illustrated in Fig. 1.

$$\phi = \cos^{-1}(1 - \varepsilon/E_2 + \varepsilon/(E_1 + E_2)) \qquad (1)$$

Here, ε is the electron rest mass energy, E_1 is the energy deposit in the forward detector, E_2 is the energy deposit in the second or rearward detector and ϕ is the Compton scatter angle provided $E_1 + E_2$ is the full incident γ-ray energy. Although the constraints of coincidence, timing and scatter angle greatly reduce the background contribution to the instrument count rate, they simultaneously reduce the detecting efficiency. Consequently, Compton telescopes are generally large in order to compensate for the reduced efficiency while retaining a high signal to noise ratio. Because of the large size, it is fortunate that Compton telescopes often have a large ratio of active to passive material. The necessity of collimation, it can be argued, is obviated by the inherent directionality of the TOF and scatter angle criteria, eliminating the mass associated with active or passive γ-ray shielding.

The basic scattering process for photons is illustrated in Fig. 1. The quantities that one measures are the position A of the Compton scatter in the forward detector, the energy E_1 of the scattered electron, the position B of the scatter in the rearward detector and the energy deposit E_2 in that detector. One computes from these quantities the direction of the scattered photon's velocity vector, i.e. the axis of the cone in Fig 1. From the energy deposits, one computes the scatter angle ϕ, the half angle of the cone and the total γ-ray

energy ($E_1 + E_2$). Without measuring the direction of the scattered electron at point A, only the polar angle of the scatter is known. From inspection one sees that the direction information suffers from an azimuthal degeneracy; that is, for a given energy, photons from any source lying on the cone mantle shown, as shown in Fig. 1, produce identical signatures in the instrument. The azimuth information is solely contained in the direction of the scattered electron in the forward detector; this direction is not measured.

3. COMPTEL Gamma Ray Response

COMPTEL, designed for the Gamma Ray Observatory, is a Compton telescope as described above. It will be the first Compton telescope to be placed on-orbit and will provide us with the opportunity to perform observations of weak cosmic sources for extended periods of time. The mechanical design of COMPTEL is illustrated in Fig. 2 (Schönfelder *et al.* 1984). An incoming γ-ray scatters off an electron in one of 7 D1 detectors and proceeds down to one of 14 D2 detectors scattering again. Such events constitute the ideal type of γ-ray interaction. The material in D1 is a liquid organic scintillator, NE213A, with the properties of low density and low Z. The detector is a fraction of a mean free path thick, meaning that the incident γ-ray (or neutron) can usually scatter in D1 and leave D1 without scattering again. For the case of small angle γ-ray scatters ($< 30°$), the incident γ-ray can deposit a large part of its energy in the D2 detector which is comprised of NaI (high density, high Z).

The liquid organic scintillator in D1 (NE213A) possesses pulse shape discrimination properties, in that proton ionization tracks produce pulses with long rise times in the emitted visible light. Conversely, electrons and other minimum ionizing particles produce pulses with short rise times. The Pulse Shape Discrimination circuit, in effect, measures this rise time, whereby the events can be, in large part, segregated into two groups, proton scatters and electron scatters. This capability of the instrument allows for efficient identification of signals from recoil or knock-on protons produced by fast neutrons scattering off hydrogen in D1. Any reaction producing a recoil proton can be identified by these means, such as inelastic scattering of fast neutrons off carbon producing a γ-ray and either a knock-on proton or neutron (which then can elastically scatter off hydrogen). Pure γ-ray producing neutron reactions off carbon in D1 are also possible and represent an intrinsic background.

The D1 and D2 subsystems of the telescope are each completely surrounded by charged particle detectors (see Fig. 2). These 4 domes of plastic scintillator NE110 are 1.5

cm thick and do not significantly attenuate the incident γ-ray or neutron fluxes, yet are virtually 100% efficient in identifying charged cosmic rays.

The incident photon direction is constrained to a cone mantle, as illustrated in Fig. 2. In order to translate this geometrical feature to the the coordinate system of the telescope we require knowledge of the positions of the γ-ray or neutron scatters in D1 and D2. This is accomplished not only by knowing in which detectors the scatters occurred, but also by using a process to locate an event within a detector by comparing the relative pulse heights of the attached photomultiplier tubes. This provides spatial information within the triggered detectors in D1 and D2.

Errors in the measured energy and scatter angle occur via uncertainties in the measured energies in D1 and D2 and uncertainties in the measured interaction positions in D1 and D2. Partial energy absorption in D2 (resulting in an escaping γ-ray) yields a low value for the total γ-ray energy and a large value for the scatter angle ϕ.

Distinguishing features of COMPTEL are summarized below.

1) Liquid scintillator NE213A is used in the upper or forward detecting array. This liquid has pulse shape discrimination properties and high light output with the chemical properties of low density and low atomic weight, minimizing multiple scattering in D1.

2) No γ-ray shields are employed. Charged particle shields provide 4π sr rejection of charged cosmic rays.

3) NaI is used in D2 for higher photopeak efficiency and better energy resolution. A high photopeak efficiency provides better angle information since less energy is lost from the system.

4) In both D1 and D2 the position of the photon (or neutron) interaction is determined via the Anger camera technique, i.e. using the relative pulse heights of the photomultiplier tubes in that module.

5) Photomultiplier tube gains are continuously monitored using standard light sources. A Light Emitting Diode in each detector module provides short term gain information, while β^- tagged ^{60}Co sources provide long term gain information with monoenergetic on-board γ-rays (Snelling *et al.* 1986).

6) The threshold of the D1 detector is nominally 50 keV providing a small scatter angle threshold, increasing total efficiency and efficiency in the on-axis direction.

7) The threshold in the D2 detection array is nominally 500 keV, which lowers the total overall energy threshold of the system to approximately 800 keV for γ-ray scatters $< 30°$.

C-2

8) A quantity related to the γ-ray scatter angle is computed on-board to determine if the event is worthy of transmission. The parameters associated with this computation are adjustable by ground command providing the capability to maximize the good event rate.

The total geometrical area of the forward detector array D1 is approximately 4300 cm^2, while the effective area for γ-ray double scatters in the range of 1 to 10 MeV is < 40 cm^2. The spatial resolution (1 σ) in a D1 module (~ 1 MeV) is ~ 2 cm, while that in a D2 module is ~ 1 cm. Although a function of incident energy and angle, the energy resolution of the system is between 5 and 10%.

COMPTEL as an imaging photon telescope relies on the full energy deposit of the γ-ray to estimate correctly the scattering angle ϕ of the photon in the instrument (Schönfelder *et al.* 1984). For a solar flare γ-ray interacting in COMPTEL the inferred scatter angle ϕ about the vector of the scattered γ-ray must be such that the photon is assigned a solar origin as indicated schematically in Fig. 2. Hence, we know that the photon deposited its full energy in the detector. The response of the telescope to such events is simple. The energy or pulse height distribution is basically Gaussian in shape with a heavily suppressed Compton tail at low energies. Since the solar γ-ray spectra are rich in continuum and lines from C, N, O, Ne, Mg etc., a simple instrumental response function will facilitate correct de-convolution of the pulse height spectra. The response of the telescope to monoenergetic photons from a ^{24}Na source is shown in Fig. 3.

The effective detector area of COMPTEL to 5 MeV solar photons incident at 30° is about 25 cm^2, decreasing to about 10 cm^2 at 1 MeV and 20 MeV (Schönfelder *et al.* 1984). For the solar γ-ray flare which occurred on 1982 December 7 we estimate that the average γ-ray flux > 1 MeV was about 1 photon cm^{-2} s^{-1} over a period of ~ 1000 s. With COMPTEL's sensitive area this would result in a count rate of 25 s^{-1}, just exceeding the telemetry rate of COMPTEL of 20 s^{-1}. For a 1000 s event duration this yields ~ 20 000 counts for good spectroscopy statistics.

4. COMPTEL Burst Measurements

The burst mode of the COMPTEL instrument can also be used to detect the first fast burst of solar γ-rays. The programmable Burst Spectrum Analyzer (BSA) continually integrates γ-ray spectra from two separate D2 detector modules in a background mode at a programmed cadence and integration time (nominally 30 s). One detector covers the energy interval from 0.1 to 1 MeV and the other the interval from 1 to 10 MeV. Each detector has an unobscured field-of-view of about 2.5 sr and an area of ~ 600 cm^2. Outside this field-of-view varying amounts of intervening material exists attenuating the solar γ-ray flux.

The capabilities of COMPTEL for burst detection are discussed by Winkler *et al.* (1986). The sequence of spectra integration is illustrated in Fig. 4. When the burst system on COMPTEL receives a signal from the Burst and Transient Source Experiment (BATSE) indicating a burst of any origin, it starts accumulating spectra in these two modules at programmed time intervals, here shown as every 1.7 s, for a total of six spectra, after which it switches to a so-called tail mode integration time of ~ 10 s as indicated schematically in Fig. 4. This fast accumulation rate provides information about the initial solar burst of γ-rays. These integration times are tentative and doubtless will be adjusted on-orbit.

5. COMPTEL Operation During Solar Flares

Within 5 s after the burst start, BATSE sends a second signal to the On-Board Computer (OBC) if the burst originated from the general direction of the Sun. Within the next two minutes, depending on the timing of the BATSE signal relative to the OBC telemetry frame, the OBC commands COMPTEL into a solar neutron mode for a time interval of 90 minutes or one orbit. In the solar neutron mode the Time-of-Flight (TOF) acceptance window for events is shifted from a (pre-flight) nominal range of - 20 ns to + 20 ns (+ corresponding to downward-moving γ-rays and neutrons) to 0 to + 40 ns. A TOF measurement of 0 ns corresponds to simultaneous events in D1 and D2 with forward-moving γ-rays having a TOF of ~ 5 ns. This change in operating mode is also shown schematically in Fig. 4. COMPTEL still accumulates spectra in two D2 detector modules, each with a geometrical area of about 600 cm^2.

Double scatter telescope events are assigned a telemetry priority depending upon the measured event characteristics. The priority γ_1 is the highest priority, reserved for cosmic γ-ray events, with other events, γ_2 priority, (e.g. neutrons) largely filling the remainder of the telemetry stream. While the instrument is in the solar neutron mode γ_1 (priority) events are still in the data stream as indicated in Fig. 4. Solar neutrons, γ_2 events, are separated from the γ-rays by pulse height requirements in D1 and D2, Pulse Shape Discrimination (PSD) in the D1 detectors and TOF criteria (Fig. 4).

6. COMPTEL Neutron Response

The ideal type of neutron interaction in COMPTEL occurs when the incoming neutron elastically scatters off a hydrogen nucleus in the D1 detector. The scattered neutron then proceeds to the D2 detector where it may interact, depositing some of its energy to produce a trigger signal as indicated in Fig. 2. The energy of the incident neutron is

computed by summing the proton recoil energy E_1 in the D1 detector with the energy of the scattered neutron E_S deduced from the TOF from the D1 to the D2 detector. The scatter angle for non-relativistic neutrons (< 150 MeV) can be computed by the formula:

$$\phi = \cos^{-1} \{E_S/(E_S+E_1)\}^{0.5}.$$

The neutron can be traced backwards from D2 to D1 through the angle ϕ to a cone mantle restricting the incident direction to include the Sun. This is a geometrical constraint identical to that of the γ-ray measurements. The pulse shape information about energy deposits in D1 is sufficient to reject more than 95% of electron recoil events greater than about 1 MeV, the energy threshold in D1 for neutron detection. This method of detecting and measuring the neutrons is clean, in that a delayed coincident scatter with the correct pulse shape in D1 is required, yielding a large signal to noise ratio. Other inelastic reactions with C also occur in the liquid scintillator, particularly at energies greater than about 50 MeV. The C interactions in D1 often produce γ-rays, deuterons or alphas which can be identified. These can be included to further increase the instrument response to neutrons. These interactions are difficult to interpret, but in the case of a solar neutron event, can be used to supplement the information obtained from the elastic scatters.

With COMPTEL in the solar neutron mode (see Fig. 4) neutron interactions appear in the γ_2 channel, covering the TOF interval from about 10 to 40 ns. The PSD and TOF criteria in this channel are such that solar neutrons incident on D1 in the energy range from about 10 MeV to 200 MeV are recorded. In this energy interval COMPTEL can observe neutrons from about 14.5 to 55 minutes after release from the Sun. This corresponds to a minimum observed delay time of 6 to 47 minutes after the onset of the γ-ray flash (assuming neutrons are not produced without accompanying γ-rays).

A prototype of COMPTEL (Science Model 3) consisting of two D1 and three D2 modules was exposed at the Indiana University Cyclotron Facility to calibrated pulsed neutron beams from 20 to 200 MeV incident at various angles to the telescope. The fluxes as measured by the beam monitor and the D1 detector in the singles mode and the flux calculated from the beam current in the cyclotron using the known neutron production cross sections agreed to within ~ 50%. The resulting data were inspected to select events obeying the proper kinematic relationship for elastic scatters. These events were then tabulated to compare with Monte Carlo calculations performed to predict the efficiencies for elastic (n,p) scattering reactions. The calculated efficiencies were systematically about 1.95 greater than those measured. This discrepancy probably arises from the various approximations used in the calculations, such as neglecting the material in front of and

internal to the telescope, underestimating the attenuation of the neutrons by C interactions in D1, and assuming that every scattered neutron incident on D2 with an energy greater than the threshold energy produces an output signal from D2. The in-flight sensitivity of COMPTEL was then modeled in the full instrument configuration. The resulting effective area of COMPTEL for neutrons incident at 30° as a function of energy is shown in Fig. 5 where the calculated area is scaled by the above factor. The heavy line indicates the calibrated energy range.

6. COMPTEL Response to the 1982 June 3 Solar γ -Ray Flare

We can use these calculated efficiencies to estimate the response of COMPTEL to the solar neutrons from a flare event such as that of 1982 June 3. The reader is referred to the paper of Lockwood *et al.* (1989) presented at the NASA/GRO Workshop from which much of this material is derived. The calculated neutron energy spectrum in total neutrons produced per MeV at the Sun as a function of neutron energy according to Murphy *et al.* (1987), assuming that the neutrons are impulsively produced, is plotted in Fig. 6. A power law in rigidity times an exponential in energy is assumed for the solar neutron production spectrum, i.e.

$$dN/dE = A\, p^{-5}\, exp(-E/1000), \qquad (2)$$

where p is in Mv and E in MeV. We further assume that the relativistic neutron energy spectrum is identical to the relativistic proton spectrum. The resulting neutron energy spectrum at the earth corrected for the neutron lifetime is also shown. The energy range of COMPTEL for solar neutrons, as indicated by the heavy line from about 10 MeV to 200 MeV, covers the maximum in the neutron energy spectrum at earth. An event such as that of 1982 June 3 would have produced about 1800 clean neutron events in COMPTEL over a time interval of about 40 minutes or an average event rate of $\leq 2\ s^{-1}$, within the telemetry bandwidth of γ_2 events.

Neutrons were detected from this event by the Solar Maximum Mission/Gamma Ray Spectrometer (SMM/GRS) (Forrest *et al.* 1980) and by ground level neutron monitors (Chupp *et al.* 1987; Debrunner *et al.* 1983; Efimov *et al.*1983). In Fig. 7 we have reproduced Fig. 1 from Chupp *et al.* (1987) showing the count rates of several energy channels of the GRS on SMM and the relative excess count rate of the Jungfraujoch neutron monitor. Chupp *et al.* (1987) state that the 56 - 199 keV X-ray channel responds predominantly to electron bremsstrahlung X-rays, while the 4.1 - 6.4 MeV photons originate largely from nuclear γ-ray line emissions indicative of energetic proton

interactions in the chromosphere and corona. In these energy bands the event started at 1142.7 UT (Forrest *et al.* 1985) and reached a maximum at 1143.5 UT. The High Energy Matrix (HEM) of the GRS responds to energy losses of > 25 MeV, a result of high energy photon and neutron interactions. The count rate of the HEM has a first peak with onset at 1143.0 UT and a maximum between 1143.0 and 1143.5 UT. A second peak is observed to start at 1145 UT, with a maximum at 1146 UT and a prolonged lower level excess count rate terminated by satellite sunset. The HEM count rate has a time structure different from those at lower energies. A fraction of this excess high-energy count rate (> 25 MeV) is due to > 50 MeV neutrons with the remainder (second peak) attributable to photon emission from charged and neutral π mesons (Forrest *et al.* 1985). The excess rate of the Jungfraujoch neutron monitor for 1 minute intervals shown in Fig. 7 is expressed in percent of the average count rate determined from the two reference intervals 1110 - 1140 UT and 1200 - 1230 UT.

The difference in the responses of the SMM detector and the Jungfraujoch neutron monitor to solar neutrons was used by Chupp *et al.* (1987) to estimate the time-averaged neutron emissivity at the Sun. Since neither the SMM detector nor the Jungfraujoch neutron monitor measure the neutron energy, the evolution of the emitted neutron spectrum in not known. One can, in the simplest case, assume either impulsive solar neutron production at a specified time or a time extended solar neutron production starting at a specified time, and following a particular intensity-time profile while maintaining a constant spectral shape at the Sun. The time-extended count rate profile seen at Jungfraujoch in Fig. 7 indicates that the solar neutron production at the Sun must have been time-extended rather than impulsive. This is supported by the conclusions of Forrest *et al.* (1985) that π meson decay produced γ-rays more than 2 minutes after the impulsive phase. In Fig. 9 we show the count rate of the SMM GRS detector and the Jungfraujoch neutron monitor (taken from Fig. 1 in Chupp *et al.* (1987)) as a function of the time of arrival of the neutrons assuming that the solar neutron production started at 1143:26 UT. Clearly, a time extended solar neutron production which has an intensity-time profile given by that of the > 25 MeV channel shown in Fig. 7 and being a power law in energy with an index of - 2.4 gives a good fit to both sets of count rates. An impulsive neutron production at 1143:26 UT also shown in Fig. 8, however, does not give a good fit to the SMM GRS and Jungfraujoch count rates. For comparison we show in the upper panel of Fig. 8 the predicted count rate ($\times$ 10) of COMPTEL to impulsive solar neutron production with the energy spectrum given by Murphy *et al.* (1987) shown in Fig. 6.

It is important to point out that since COMPTEL measures the solar neutron energies directly, a neutron energy spectrum at earth can be constructed. For impulsive

neutron production at the Sun with the neutron energy spectrum shown in Fig. 6, COMPTEL would have measured the spectrum shown in Fig. 9.

7. Conclusions

During a two year period after mid-1990, the projected launch date for GRO, we should expect a large number of solar γ-ray events with emission of photons > 0.8 MeV. From February 1980 to December 1982 Rieger *et al* (1983) found ~ 130 solar flares with emission > 0.3 MeV, of which 8 emitted > 10 MeV γ-rays. Two of these events emitted measurable neutrons > 50 MeV. Consequently, we should expect to find many solar flares with both high energy γ-rays (> 1 MeV) and neutrons (> 10 MeV) present, since the energy threshold of COMPTEL for neutrons is much lower than that of the SMM detector and since the neutron response curve of COMPTEL is well-matched to the solar neutron energy spectrum at earth.

By combining the normal imaging capabilities of COMPTEL with its burst mode operation and solar neutron spectroscopic abilities, definitive information should be obtained about the spectral evolution of nucleonic and electronic processes in solar flares. Neutron energy measurements provide more precise and extensive data about proton acceleration. For the unusual solar flare occurring on the west limb of the Sun in which prompt, energetic solar protons (> 500 MeV), γ-rays and neutrons are observed and measured, we should be in a position to understand better the relative roles of stochastic and diffusive shock acceleration processes at the Sun.

Acknowledgements

The COMPTEL experiment is the result of the efforts of the Max Planck Institut für Extraterrestrische Physik, Garching, FRG; the Space Research Organization of the Netherlands, Leiden, The Netherlands; the University of New Hampshire, Durham, New Hampshire and the Space Science Department of ESA/ESTEC, Noordwijk, The Netherlands. The work of the authors has been funded by NASA contract NAS5-26645.

References

Chupp, E. L., H. Debrunner, E. Flückiger, D. J. Forrest, F. Golliez, G. Kanbach, W. T. Vestrand, J. Cooper, and G. Share 1987, *Ap. J.*, **318** : 913-925.

Debrunner, H., E. Flückiger, E. L. Chupp, and D. J. Forrest 1983, *Proc. 18th Internat. Cosmic Ray Conf.*, **4** : 75.

Efimov, Yu E., G. E. Kocharov, and K. Kudela 1983, *Proc. 18th Internat. Cosmic Ray Conf.*, **10** : 276.

Forrest, D. J., E. L. Chupp, J. M. Ryan, M. L. Cherry, I.U. Gleske, C. Reppin, K. Pinkau, E. Rieger, G. Kanbach, R. L. Kinzer, G. Share, W. N. Johnson, and J. D. Kurfess 1980, *Solar Phys.*, **65** : 15-23.

Forrest, D. J., W. T. Vestrand, E. L. Chupp, E. Rieger, J. Cooper, and G. Share 1985, *Proc. 19th Internat. Cosmic Ray Conf.*, **4** : 146-149.

Lockwood, John, V. Schönfelder, K. Bennett, G. Eymann, J. M. Ryan, D. Morris, J. Macri, and B. Swanenburg 1989, to be published in Proceedings of GRO Workshop, Greenbelt MD.

Murphy, R. J., C.D. Dermer, and R. Ramaty 1987, *Ap. J.*, **316** : L41-56.

Rieger, E., C. Reppin, G. Kanbach, D. J. Forrest, E. L. Chupp, and G. H. Share 1983, *Proc. 18th Internat. Cosmic Ray Conf.*, **10** : 338.

Schönfelder, V., R. Diehl, G. Lichti, H. Steinle, B. N. Swanenburg, A. Deerenberg, H. Aarts, J. A. Lockwood, W. R. Webber, J. M. Ryan, G. Simpson, B. G. Taylor, K. Bennett, and M. Snelling 1984, *IEEE Trans. Nucl. Sci.*, **NS-31** (1) : 766-770.

Snelling, M., K. Bennett, and J. Clear 1986, *Nucl. Instr. Meth.*, **A248** : 545-549.

Winkler, C., V. Schönfelder, R. Diehl, G. Lichti, H. Steinle, B.N. Swanenburg, H. Aarts, A. Deerenberg, W. Hermsen, J. A. Lockwood, J. M. Ryan, G. Simpson, W. R. Webber, K. Bennett, A. v. Dordrecht, and B.G. Taylor 1986, *Adv. Space Res.*, **6** (4) : 113-117.

Figure Captions

1. The kinematics of a Compton scatter, the principle of measurement for a Compton telescope.

2. The mechanical structure of COMPTEL, illustrating the detection method for γ-rays and neutrons.

3. The energy response of COMPTEL to 1.37 and 2.75 MeV photons under the conditions of ideal scattering kinematics, i.e. ϕ is the true scatter angle.

4. The sequence of spectra integrations of the COMPTEL burst system. Shown is the *Background*, *Burst* and *Tail* spectra integrations relative to the trigger signal from BATSE. Also shown are the time-of-flight spectra used during normal operations and during solar flare measurements. The function of γ_1 and γ_2 event data is illustrated on the lower part of the figure.

5. COMPTEL effective area for neutron detection at 30° incident angle. The solid line indicates the calibration range.

6. The time integrated neutron spectrum at the Sun (Murphy *et al.* 1987) and at earth.

7. Intensity-time profiles of several GRS data channels and count rate of Jungfraujoch neutron monitor, reproduced from Chupp *et al.* (1987).

8. Count rates of the SMM/GRS data and Jungfraujoch neutron monitor superimposed on the predicted count rate for COMPTEL for the same event, assuming both impulsive and extended emissions of neutrons.

9. Predicted COMPTEL count rate spectrum due to a neutron flux as illustrated in Fig. 6.

PRINCIPLE OF MEASUREMENT

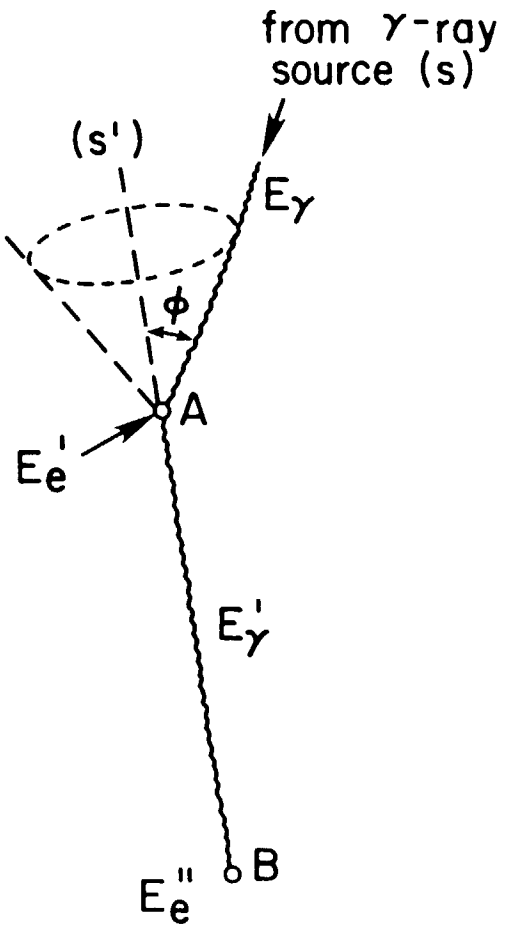

if $E_\gamma' = E_e''$

$\Longrightarrow$

$$E_\gamma = E_e' + E_e''$$

$$\cos\phi = 1 - \frac{m_0c^2}{E_e''} + \frac{m_0c^2}{E_e' + E_e''}$$

Figure 1

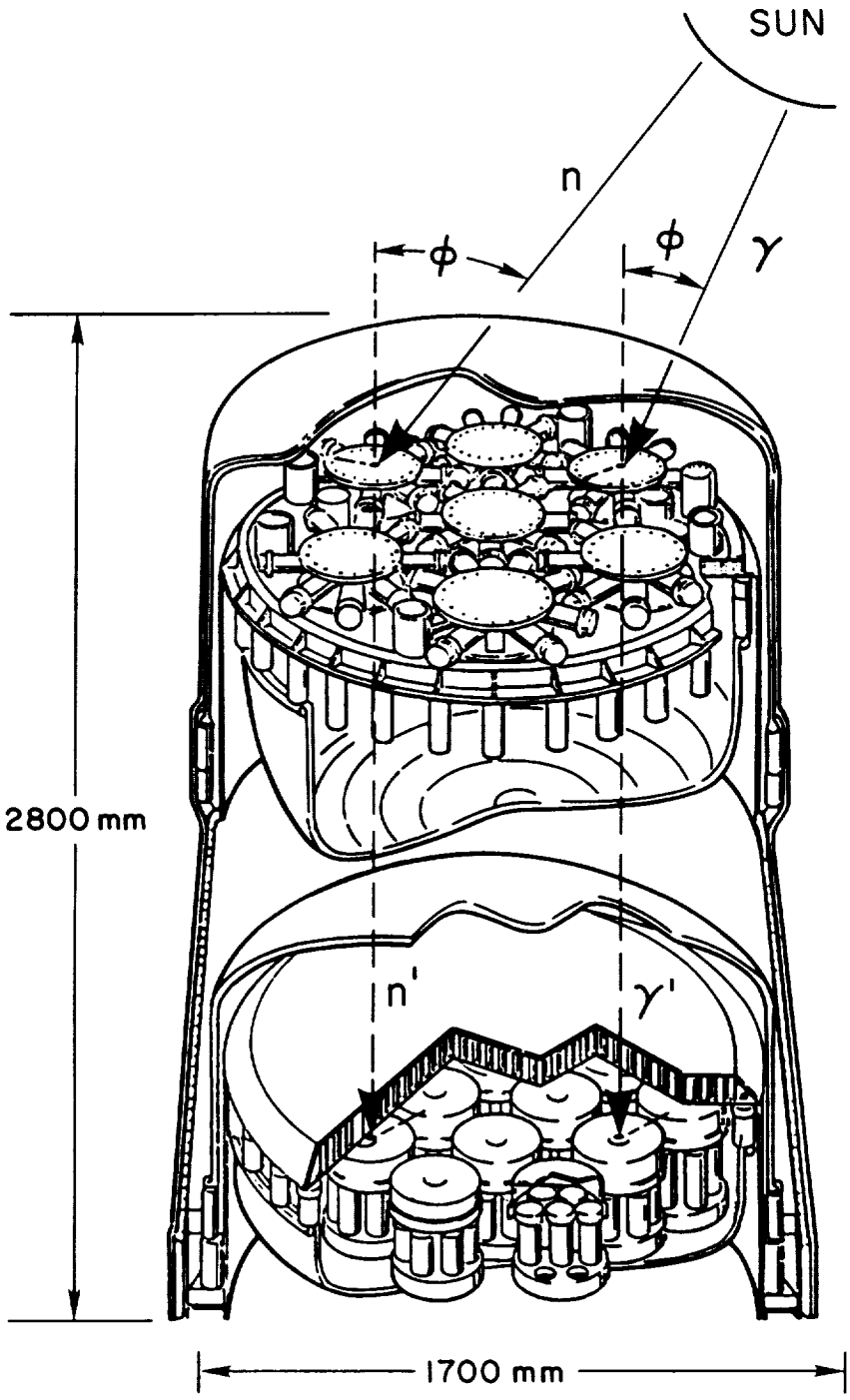

COMPTEL

IMAGING COMPTON TELESCOPE

Figure 2

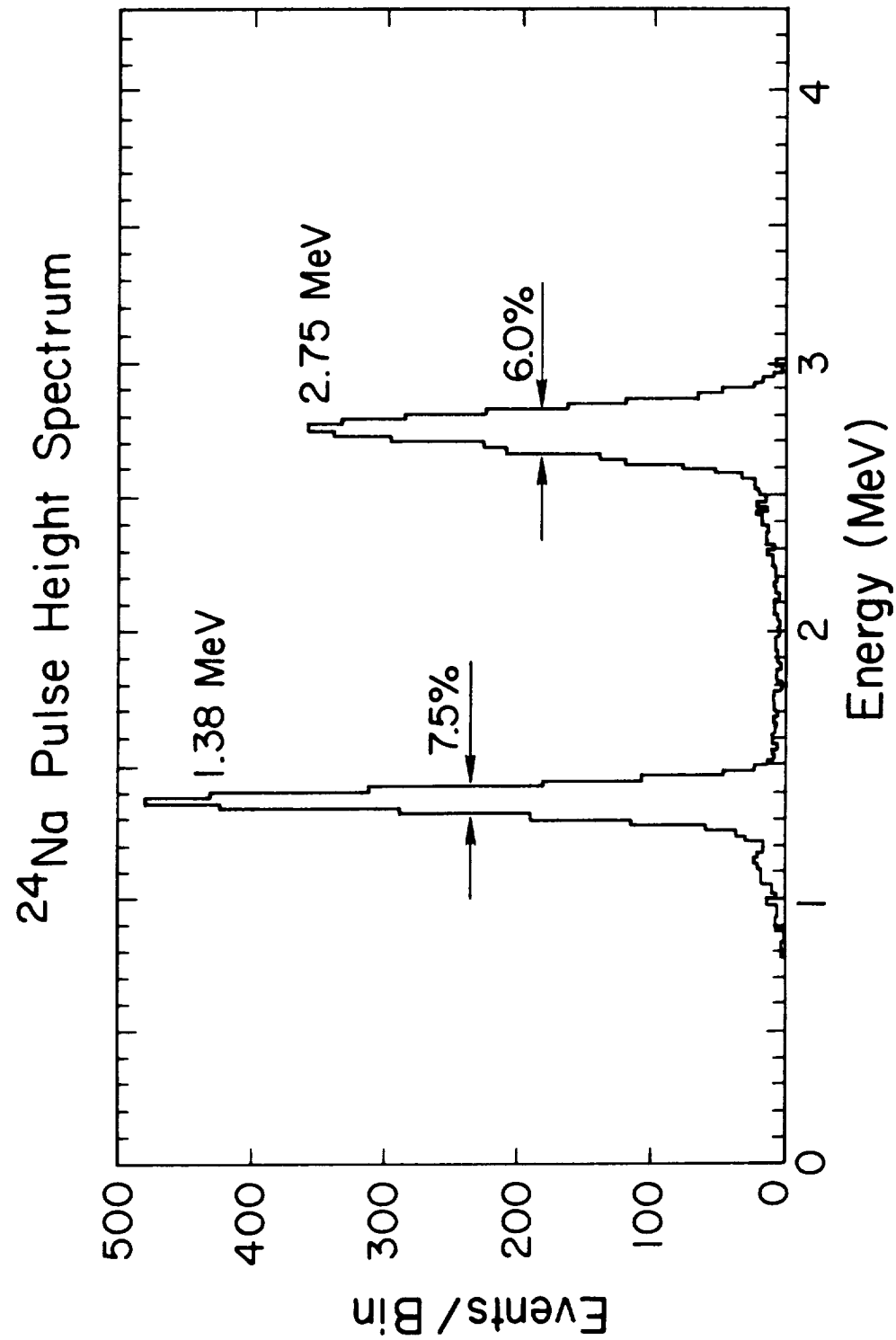
^{24}Na Pulse Height Spectrum
1.38 MeV
7.5%
2.75 MeV
6.0%
Events / Bin
Energy (MeV)
0
100
200
300
400
500
1
2
3
4

Figure 3

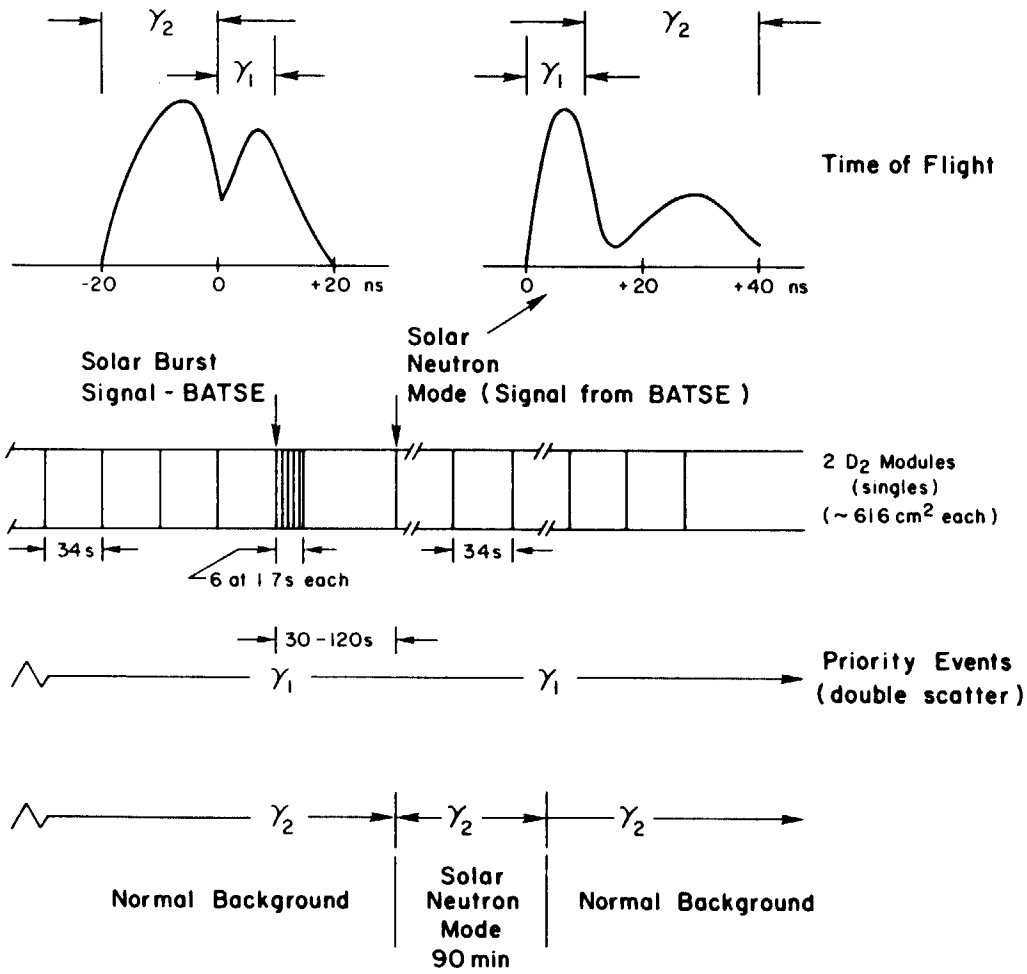
γ_2
γ_1
γ_1
γ_2
Time of Flight
-20
0
+20 ns
0
+20
+40 ns
Solar
Neutron
Mode (Signal from BATSE)
Solar Burst
Signal - BATSE
2 D_2 Modules
(singles)
(~ 616 cm^2 each)
34 s
6 at 1 7s each
34 s
30 - 120s
γ_1
γ_1
Priority Events
(double scatter)
γ_2
γ_2
γ_2
Normal Background
Solar
Neutron
Mode
90 min
Normal Background

Figure 4

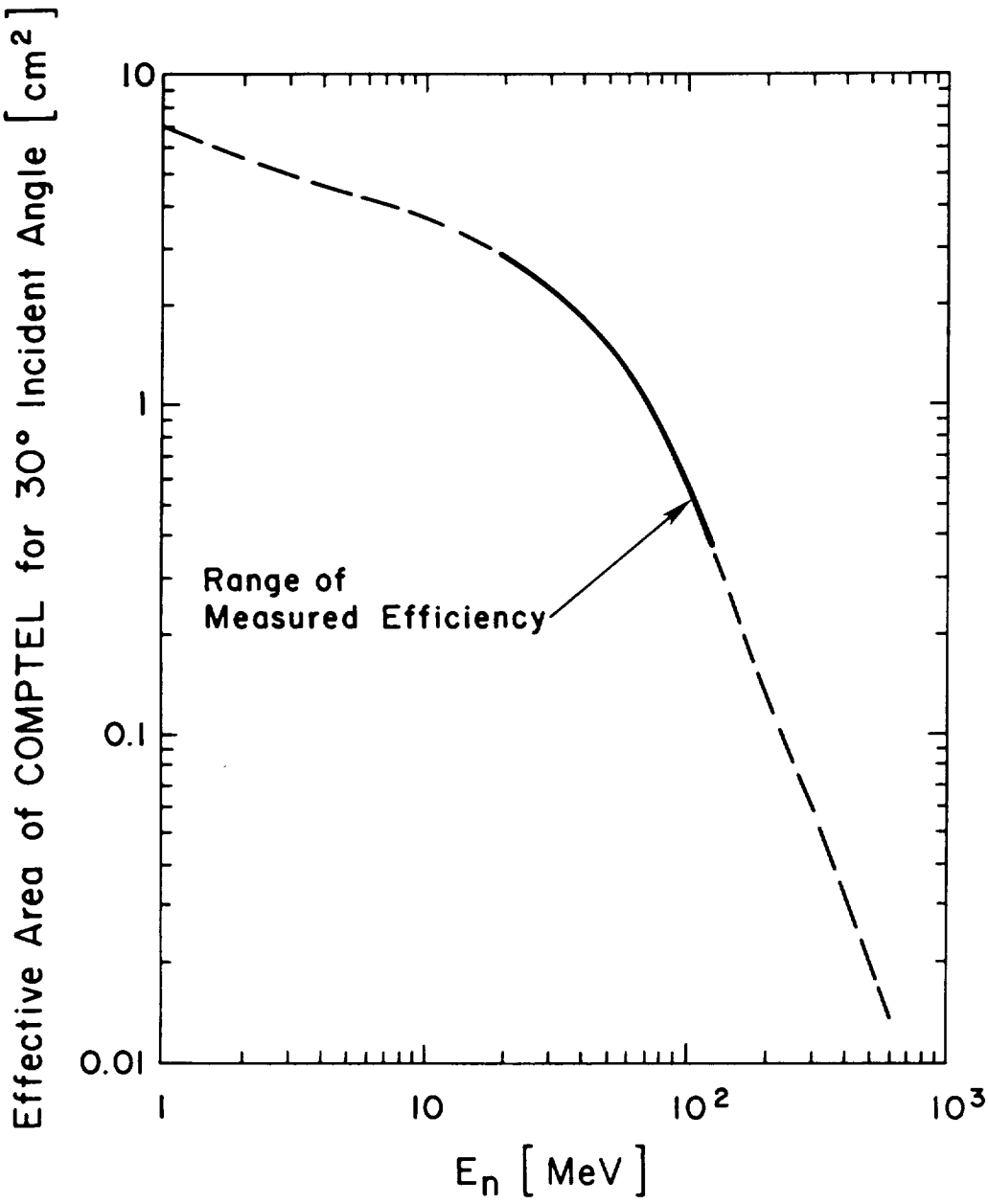
Effective Area of COMPTEL for 30° Incident Angle [cm²]
10
1
0.1
0.01
Range of
Measured Efficiency
1
10
10²
10³
E_n [MeV]

Figure 5

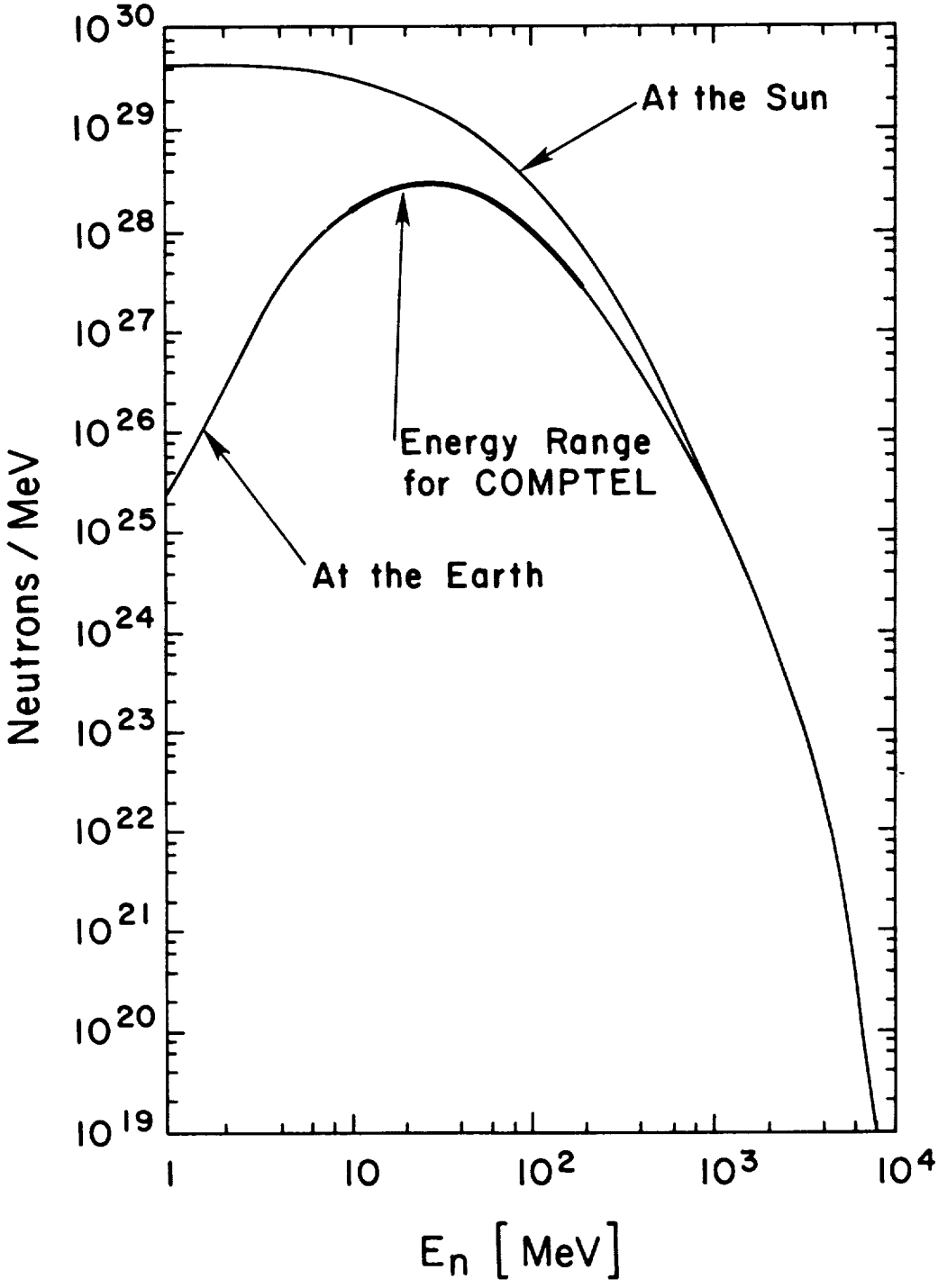
10^{30}
10^{29}
10^{28}
10^{27}
10^{26}
10^{25}
10^{24}
10^{23}
10^{22}
10^{21}
10^{20}
10^{19}
Neutrons / MeV
At the Sun
Energy Range
for COMPTEL
At the Earth
1
10
10^2
10^3
10^4
E_n [MeV]

Figure 6

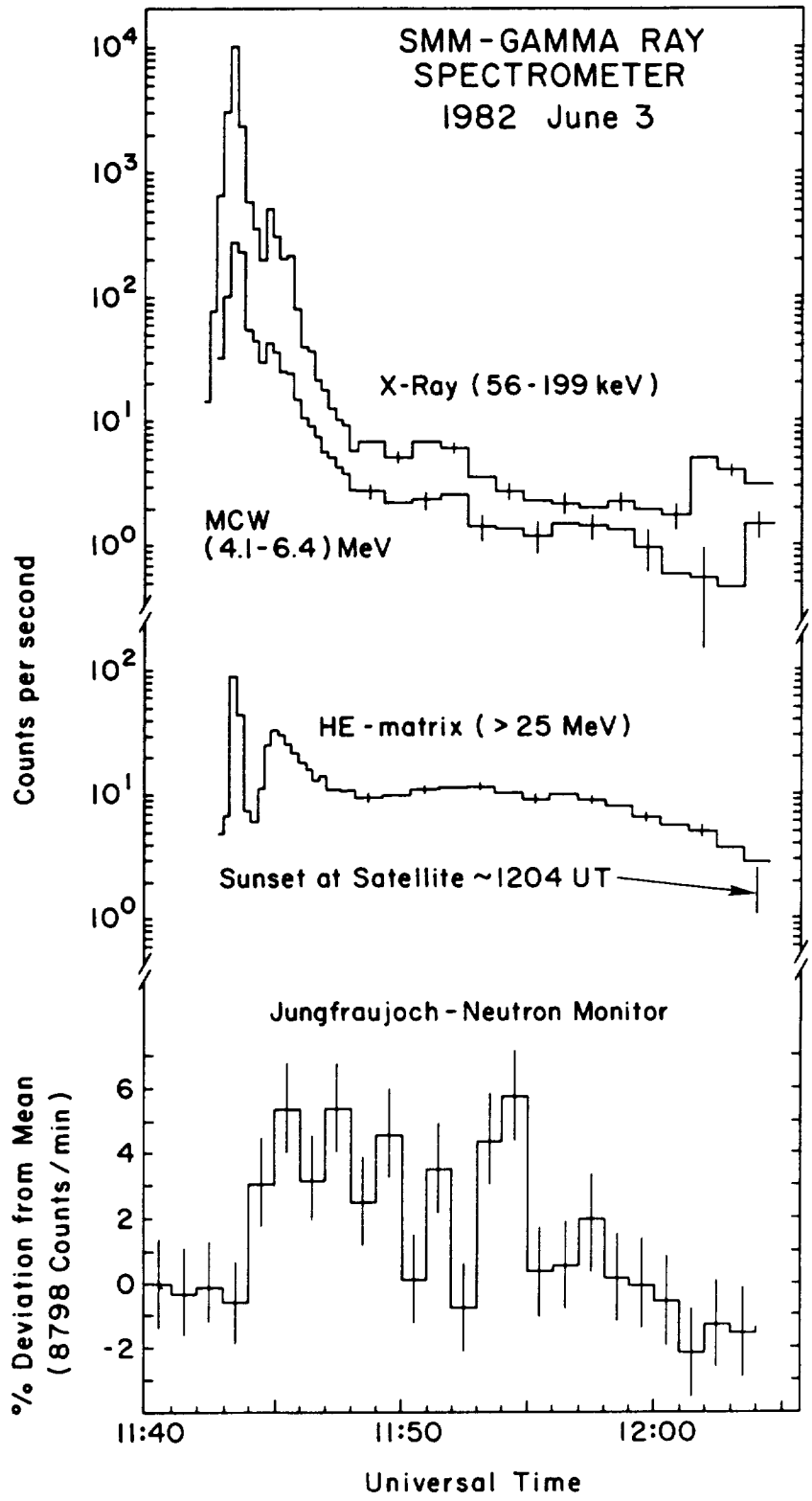

From Figure 1 in Chupp et al. (1987)

Figure 7

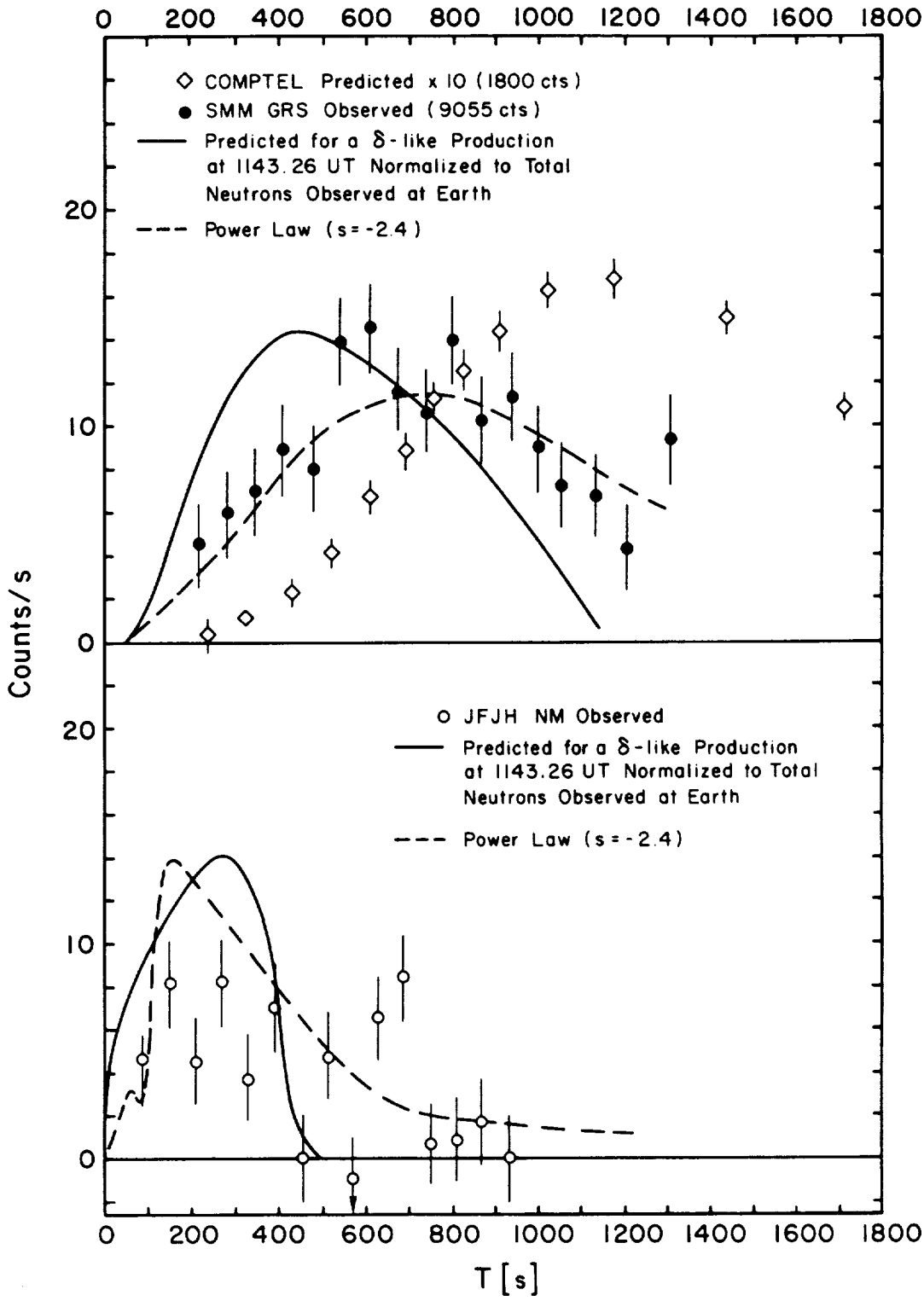
0 200 400 600 800 1000 1200 1400 1600 1800
◇ COMPTEL Predicted x 10 (1800 cts)
● SMM GRS Observed (9055 cts)
Predicted for a δ-like Production at 1143.26 UT Normalized to Total Neutrons Observed at Earth
Power Law (s=-2.4)
20
10
0
Counts/s
o JFJH NM Observed
Predicted for a δ-like Production at 1143.26 UT Normalized to Total Neutrons Observed at Earth
Power Law (s=-2.4)
20
10
0
0 200 400 600 800 1000 1200 1400 1600 1800
T [s]

Figure 8

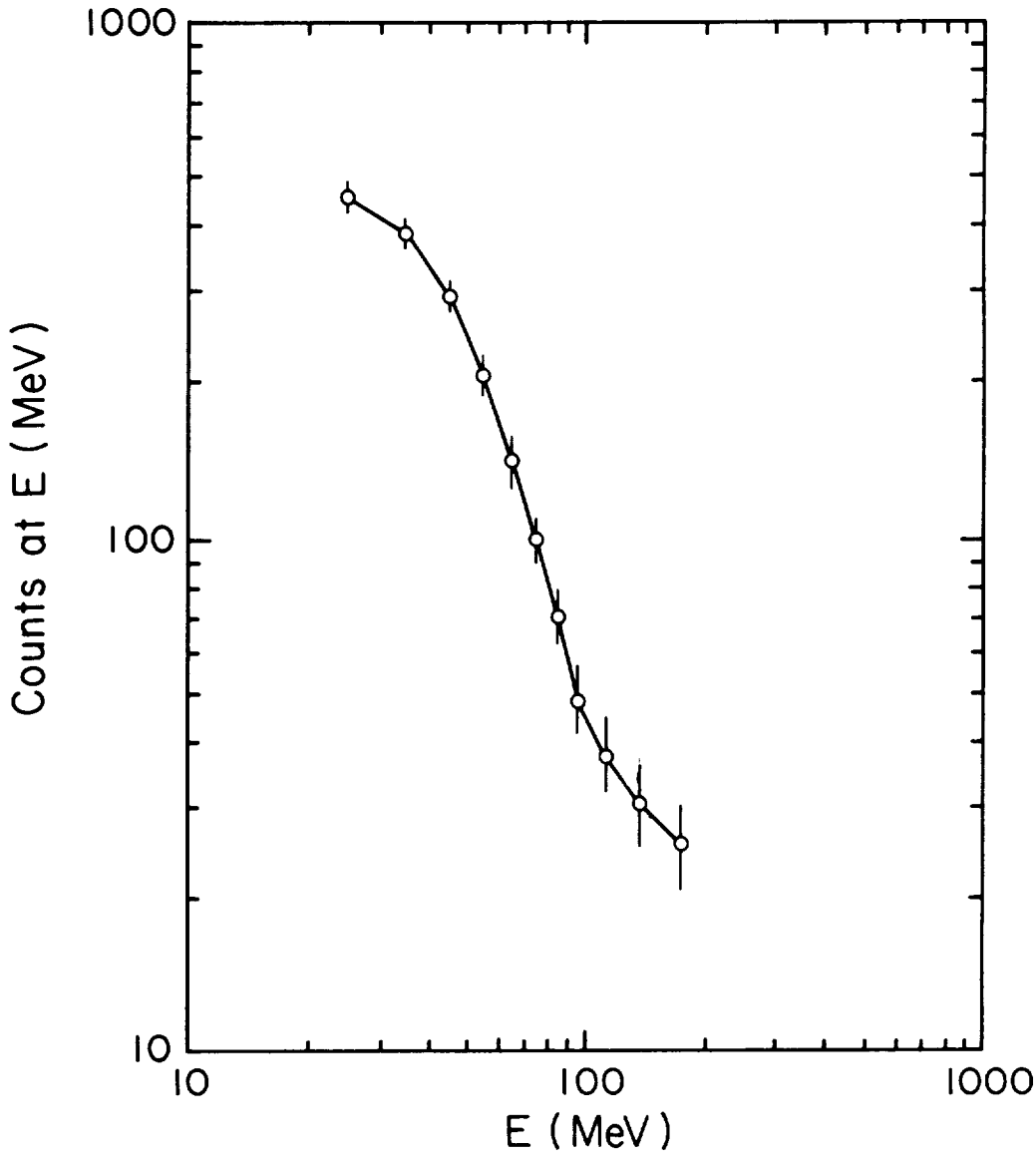

Figure 9